Int. J. Solids Structures Vol. 25, No. 3, pp. 299–326, 1989
Printed in Great Britain.

0020-7683/89 $3.00 + .00

A PLASTIC-DAMAGE MODEL FOR CONCRETE

J. LUBLINER
Department of Civil Engineering, University of California, Berkeley, California, U.S.A.

and

J. OLIVER, S. OLLER and E. OÑATE
Universitat Politècnica de Catalunya, E.T.S. Ingenieros de Caminos, Canales y Puertos, Barcelona, Spain

(*Received* 6 *April* 1988; *in revised form* 6 *August* 1988)

Abstract—In this paper a constitutive model based on an internal variable-formulation of plasticity theory for the non-linear analysis of concrete is presented. The model uses a new yield criterion which matches experimental data quite well and it accounts for both elastic and plastic stiffness degradations effects. Onset and amount of cracking can be studied by a simple postprocessing of the finite-element plasticity solution. The accuracy of the model is checked with some examples of application.

1. INTRODUCTION

The classical theory of plasticity, like any mathematical representation of the mechanical behavior of solids, may be viewed in two ways: as a translation of physical reality, and as a model that approximates the behavior under certain circumstances. The first view is often held with regard to ductile crystalline solids, especially metals, although the attempts to relate mathematical plasticity theory to dislocations have not been markedly successful. With regard to concrete and rock, however, it has generally been acknowledged that such prominent features of plasticity theory as a well defined yield criterion and strictly elastic unloading are approximations at best. Nevertheless, many problems involving these materials have been quite successfully treated by means of plasticity theory, and these results are not invalidated by fact that other problems have not been so successfully treated, nor by the fact that other models may have been equally effective.

The broadest area of success of plasticity theory with concrete is the treatment of reinforced concrete (see Chen, 1982 for a survey of the results) and other situations in which the material acts primarily in compression. In problems in which tension, with the attendant crack development, plays a significant role—such as shear failure in reinforced-concrete structures—the usual procedure nowadays is to apply plasticity theory in the compression zone, and treat the zones in which at least one principal stress is tensile by one of several versions of fracture mechanics, such as: linear elastic fracture mechanics, Bežant and Cedolin (1980); smeared-crack models, Rashid (1968), Suidan and Schnobrich (1973), de Borst and Nauta (1984); the fictitious-crack model, Hillerborg *et al.* (1976); and crack-band theory, Bažant and Oh (1983).

In spite of the success of this approach in solving numerous problems, it presents some inconvenient features that limit its usefulness, such as the need for defining uncoupled behavior along each principal stress (or strain) direction, the use of a quite arbitrary shear retention factor to ensure some shear resistance along the crack, the lack of equilibrium at the cracking point when more than one crack is formed (Oñate *et al.*, 1986), the difficulties of defining stress paths following the opening and closing of cracks under cyclic loading conditions, and the difficulties of dealing with the combined effect of cracking and plasticity at the damaged points (de Borst, 1987).

Some of these limitations could be avoided if a single constitutive model could be used that governs the non-linear behavior of concrete, including failure, in both tension and compression, with appropriate allowance made for the different values of the parameters describing the two modes. It is the purpose of this paper to formulate such a model in the

form of a theory of plasticity. It must be recognized at the outset, however, that not all non-linear behavior of concrete, rock and similar materials is represented by permanent (plastic) deformation: at least in the early stages, it may be caused primarily by stiffness degradation, and the model must take this into account.

As is well known, concrete and geomaterials eventually exhibit strain-softening, leading to a complete loss of strength, under all stress processes other than triaxial compression in which the hydrostatic pressure predominates over the stress deviator. In particular, strain-softening occurs in both simple tension and simple compression. While strain-softening in tension is naturally described in the models based on fracture mechanics, strain-softening in compression is controversial (Read and Hegemier, 1984). However, the localization and mesh-sensitivity associated with strain-softening occur in tension and compression alike. In fact, the qualitative behavior of concrete and many rocks is not significantly different in tension and compression. In this regard they resemble such materials as cohesive soils, and may be classed with them as *frictional materials with cohesion*. The eventual loss of strength may be thought of as the vanishing of the cohesion.

The essential elements of any model based on classical plasticity theory are the *yield criterion*, the *flow rule* and the *hardening rule*, the last to be interpreted in a broad sense so that both hardening and softening may be accounted for, and to be identified with the evolution equations of the internal variables contained in the yield criterion. For such a model to be capable of representing the behavior of a material such as has been described, the yield criterion must be of a form in which the concept of cohesion is unambiguously defined, and the hardening rule must be such as to lead to the vanishing of the cohesion.

The first of these objectives is met by the Mohr–Coulomb and Drucker–Prager yield criteria, which have the form

$$F(\sigma) = c, \tag{1}$$

where $F(\sigma)$ is a function of the stress components that is *homogeneous of the first degree*, and c may be identified with the cohesion or some constant multiple thereof. These criteria, however, do not represent experimental results for concrete or rocks very well unless they are suitably modified (Read and Hegemier, 1984; Oñate *et al.*, 1987, 1988). In recent years numerous yield and failure surfaces for concrete have been proposed: Chen and Chen (1975), Ottosen (1977), Chen (1982), Podgórski (1985), Fardis and Chen (1986), Klisiński and Mróz (1987), Dvorkin *et al.* (1987). Very few of them, however, have the form described above.

When a yield criterion of the form of eqn (1) has been found, the second objective of the model may be met if the evolution of the cohesion c is determined by a *plastic-damage variable* which resembles the *hardening variable* of the isotropic hardening rule of classical plasticity in that it never decreases, and it increases if and only if plastic deformation takes place. However, strain-softening requires that the cohesion decrease after a maximum value (for which eqn (1) represents the *failure surface*) has been reached, and that it vanishes when the plastic-damage variable attains a critical value.

A model meeting the aforementioned objectives, based on a simple modification of classical Mohr–Coulomb plasticity, has been previously presented by the authors (Oñate *et al.*, 1987, 1988). It is the purpose of this paper to present an improved model of this type based on an internal-variable formulation of plasticity theory, and with a new yield criterion that matches experimental data for concrete quite well. The model will be described and discussed in Section 2, with elastic stiffness degradation, however, neglected. An extension of the model to account for stiffness degradation will be presented in Section 3. Computational implications of the model, with numerical solutions of illustrative problems, will be discussed in Section 4.

2. THE PLASTIC-DAMAGE MODEL WITHOUT STIFFNESS DEGRADATION

2.1. *General features*

As described in the Introduction, the plastic-damage model is a form of classical plasticity theory in which the usual "hardening variable" is replaced by a *plastic-damage*

variable κ, similar to the former in that it never decreases, and increases if and only if plastic deformation takes place. However, the plastic-damage variable cannot increase beyond a limiting value, and the attainment of this value at a point of the solid represents *total damage*, which can be interpreted as the formation of a macroscopic crack. The variable κ can be non-dimensionalized so that its maximum value is unity.

As was also said, the model is intended to apply to frictional materials, in which total damage is assumed to correspond to the *vanishing of the cohesion*. The yield criteria most often used for such materials are the Mohr–Coulomb and Drucker–Prager criteria, both of which may be written in the form

$$F(\sigma) = c, \tag{2}$$

where c is the cohesion, and $F(\sigma)$ is a function that is homogeneous in the first degree in the stress components. However, both these yield criteria have notoriously poor correlation with experimental data for concrete and geomaterials. Numerous improvements to these yield criteria have been proposed in recent years: Chen and Chen (1975), Ottosen (1977), Chen (1982), Podgórski (1985), Fardis and Chen (1986). However, they do not take the form of eqn (2) with $F(\sigma)$ a homogeneous function of the stress components, and consequently do not permit an unambiguous definition of the cohesion. A first attempt of the authors to obtain suitable yield criteria for concrete in the form of eqn (2) was to modify the Mohr–Coulomb criterion to fit experimental data. Numerical results obtained in the finite-element analysis of various concrete structures using the framework of standard plasticity theory were encouraging and motivated the present research. A new yield criterion of the form (2), whose fit with experimental data is about as good as that of any other proposed criterion (except possibly in the domain of high hydrostatic pressures) will be presented in Section 2.4.

The cohesion c will be scaled so that its initial value is f_{c0}, the initial yield strength in uniaxial compression, which may be identified with the "discontinuity" stress, i.e. the stress at which the volume strain attains its extremum. Consequently $c = f_{c0}$ when $\kappa = 0$ and $c = 0$ when $\kappa = 1$. However, unlike the usual plasticity models with isotropic hardening, c is not necessarily taken simply as a function of κ. Rather, the value of c at a given κ may depend on the process—that is, the cohesion c is itself assumed to be an internal variable, governed by a rate equation in which $\dot{c}$ is proportional to $\dot{\kappa}$, the proportionality factor being a function of the state variables.

If degradation of the elastic stiffness is not taken into account, and if the elastic stiffness tensor is denoted by $\mathbf{D}$, then the governing equations of the model consist of: (a) the *yield criterion* (2); (b) the *elastic–plastic strain decomposition*

$$\varepsilon = \mathbf{D}^{-1}\sigma + \varepsilon^{\mathrm{p}}; \tag{3}$$

(c) the *flow rule*

$$\dot{\varepsilon}^{\mathrm{p}} = \dot{\lambda}\mathbf{g}, \tag{4}$$

where $\dot{\lambda}$ the plastic loading factor and $\mathbf{g} = \partial G/\partial\sigma$ is the plastic flow vector normal to the plastic potential surface $G = \text{const}$; (d) the *rate equation for* κ, which will be assumed to be of the form

$$\dot{\kappa} = \mathbf{h}^{\mathrm{T}}(\sigma, c, \kappa)\dot{\varepsilon}^{\mathrm{p}}; \tag{5}$$

and (e) the *rate equation for* c, of the form

$$\dot{c} = k(\sigma, c, \kappa)\dot{\kappa}. \tag{6}$$

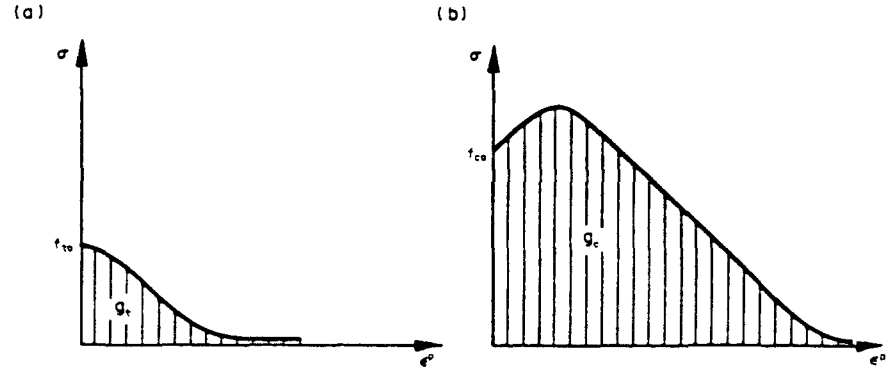

Fig. 1. Uniaxial curves (σ–ε^p): (a) tension; (b) compression.

2.2. *Definition of* κ

Uniaxial stress states. Let us suppose that we have available experimentally derived stress–strain diagrams in uniaxial tension and compression, and that these may be converted into σ–ε^p curves, as in Fig. 1. Let us further assume that the areas under these curves are finite and equal to g_t and g_c, respectively. For the tension test, let us define

$$\kappa = \frac{1}{g_t}\int_0^{\varepsilon^p} \sigma \, d\varepsilon^p. \tag{7}$$

With κ as the independent variable, curve (a) of Fig. 1 may further be converted into a function $\sigma = f_t(\kappa)$, such that $f_t(0) = f_{t0}$ and $f_t(1) = 0$. Similarly, for the compression test we may define

$$\kappa = \frac{1}{g_c}\int_0^{\varepsilon^p} \sigma \, d\varepsilon^p \tag{8}$$

and convert curve (b) of Fig. 1 into $\sigma = f_c(\kappa)$ such that $f_c(0) = f_{c0}$ and $f_c(1) = 0$.

An analytically convenient function $f(\kappa)$ that may serve as either $f_c(\kappa)$ or $f_t(\kappa)$ and which is consistent with the fact that experimentally observed stress–strain curves tend to attain the zero-stress level asymptotically (rather than at a finite "ultimate strain") may be derived from the σ–ε^p relation given by

$$\sigma = f_0[(1+a)\exp(-b\varepsilon^p) - a\exp(-2b\varepsilon^p)],$$

where a and b are dimensionless constants that may be obtained if $g = \int_0^{\infty} \sigma \, d\varepsilon^p$ and $(d\sigma/d\varepsilon^p)|_{\varepsilon^p=0}$ are given:

$$g = \frac{f_0}{b}\left(1 + \frac{a}{2}\right),$$

$$\left.\frac{d\sigma}{d\varepsilon^p}\right|_{\varepsilon^p=0} = f_0 b(a-1).$$

Note that $a > 1$ implies initial hardening, while $a < 1$ implies softening immediately after yielding.

By integration we obtain

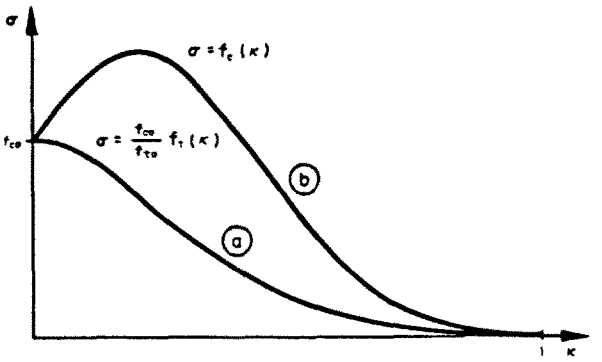

Fig. 2. Uniaxial curves (σ–κ): (a) tension; (b) compression.

$$\kappa = \frac{1}{g}\int_0^{\varepsilon^p} \sigma \, d\varepsilon^p = 1 - \frac{1}{2+a}[2(1+a)\exp(-b\varepsilon^p) - a\exp(-2b\varepsilon^p)],$$

so that, for $a \neq 0$,

$$\exp(-b\varepsilon^p) = \frac{1}{a}[1+a-\sqrt{1+a(2+a)\kappa}],$$

and therefore

$$\sigma = f(\kappa) = \frac{f_0}{a}[(1+a)\sqrt{\phi(\kappa)} - \phi(\kappa)],$$

where $\phi(\kappa) = 1+a(2+a)\kappa$. If $a > 1$, then $f(\kappa)$ attains a maximum value of $f_m = f_0(1+a)^2/4a$, or

$$a = 2(f_m/f_0) - 1 + 2\sqrt{(f_m/f_0)^2 - (f_m/f_0)}.$$

The significance of g_t and g_c. It has been made abundantly clear over the past decade that the strain-softening branch of the stress–strain curves of concrete and rock cannot represent a local physical property of the material. The arguments have been advanced both on physical grounds and on the basis of the mesh-sensitivity of numerical solutions obtained by means of the finite-element method. The mesh-sensitivity can be largely eliminated if one defines $g_t = G_t/l$ and $g_c = G_c/l$, where l is a characteristic length related to the mesh size, and G_t and G_c are quantities with the dimensions of energy/area that are *assumed* to be material properties.

In problems involving tensile cracking, G_t may be identified with the specific fracture energy G_f, defined as the energy required to form a unit area of crack. It has generally been assumed that G_f is a true material property, and methods have been developed for determining it (Rots *et al.*, 1985). For the characteristic length l, various approaches have been proposed: Bažant and Oh (1983), Crisfield (1986), Cervera *et al.* (1987), Oliver (1988).

Not so much attention has been paid to the corresponding compressive problem. Compressive failure may occur through several mechanisms—crushing, shearing, and transverse cracking—and consequently G_c, if it is indeed a material property, cannot readily be identified with any particular physical energy. Moreover, it must be kept in mind that it is only the descending portion of the stress–strain curve that is mesh-sensitive. Consequently, a consistent definition of g_c must take the form $g_{c0} + g_{c1}$, where g_{c0} is the area under the σ–ε^p curve up to the peak stress, and g_{c1} is the remainder. Now, g_{c0} is mesh-independent and is therefore a material property. For g_{c1} we postulate, for convenience, that $g_{c1} = G_{c1}/l_t$, where l is the forementioned mesh-dependent characteristic length for tensile cracking, and

G_{c1} is an assumed material property chosen in such a way that the numerical analysis of a standard compression test gives results that coincide with experimental data.

Multiaxial stress states. In attempting to extend the preceding definitions to multiaxial stress states, we consider first pure (but not necessarily uniaxial) tension and compression states; that is, if the principal stresses σ_1, σ_2, σ_3 are ordered such that $\sigma_1 \geqslant \sigma_2 \geqslant \sigma_3$, then either $\sigma_3 \geqslant 0$ (pure tension) or $\sigma_1 \leqslant 0$ (pure compression).

More specifically, consider biaxial compression, i.e. $\sigma_1 = 0$. It is tempting to use the total energy dissipated, $\int(\sigma_3 \mathrm{d}\varepsilon_2^p p + \sigma_3 \mathrm{d}\varepsilon_3^p)$, suitably normalized, as a damage variable. However, experiments by Kupfer *et al.* (1969) and Tasuji *et al.* (1978) indicate that even $\int(\sigma_3 \mathrm{d}\varepsilon_3^p$ alone is greater in the biaxial than in the uniaxial case, if ε_3^p is identified with the offset strain (total strain less extrapolated elastic strain, allowing for stiffness degradation). Moreover, on the σ_3–ε_3 curves, the peak stress occurs at a value of the ε_3^p that is approximately independent of the stress-component ratio σ_3/σ_2. Consequently the area under the σ_3–ε_3^p curve up to the peak is approximately proportional to the ratio $|\sigma_3|_{\max}$ to the uniaxial value f_{cm} (conventionally denoted f_c'). In order that the value of κ corresponding to the peak stress may be the same in the biaxial as in the uniaxial compression case, the definition (8) cannot be used in the biaxial case either. An alternative definition of κ, which reduces (8) in the uniaxial case, is embodied in the rate equation

$$\dot{\kappa} = -\frac{1}{g_c} f_c(\kappa)\dot{\varepsilon}_3^p. \tag{9}$$

Analogously, in pure multiaxial tension we can assume that

$$\dot{\kappa} = \frac{1}{g_t} f_t(\kappa)\dot{\varepsilon}_1^p. \tag{10}$$

Finally, we consider a state of stress that is neither pure tension nor pure compression, i.e. $\sigma_1 > 0$ and $\sigma_3 < 0$ (for example, simple shear). We need an equation for κ whose right-hand side tends to that of eqn (9) or (10) as $\sigma_3 \to 0$ or $\sigma_1 \to 0$, respectively. Such an equation may be deduced from the more general equation, presumably valid at all stress states,

$$\dot{\kappa} = \frac{r(\boldsymbol{\sigma})}{g_t} f_t(\kappa)\dot{\varepsilon}_1^p - \frac{1-r(\boldsymbol{\sigma})}{g_c} f_c(\kappa)\dot{\varepsilon}_3^p, \tag{11}$$

where $r(\boldsymbol{\sigma})$ is a weight factor depending continuously on $\boldsymbol{\sigma}$ such that $0 \leqslant r(\boldsymbol{\sigma}) \leqslant 1$, with $r(\boldsymbol{\sigma}) = 1$ if $\sigma_i \geqslant 0$ for all i, $i = 1, 2, 3$, and $r(\boldsymbol{\sigma}) = 0$ if $\sigma_i \leqslant 0$ for all i. A particular form of $r(\boldsymbol{\sigma})$ is

$$r(\boldsymbol{\sigma}) = \frac{\sum_{i=1}^{3} \langle \sigma_i \rangle}{\sum_{i=1}^{3} |\sigma_i|}, \tag{12}$$

where $\langle x \rangle = \frac{1}{2}(|x| + x)$. The special cases of pure tension and compression follow obviously from eqn (12). For biaxial tension–compression ($\sigma_1 > 0$, $\sigma_2 = 0$, $\sigma_3 < 0$), eqn (12) yields the following rate equation for κ:

$$\dot{\kappa} = \frac{1}{g_t} \frac{\sigma_1}{\sigma_1 - \sigma_3} f_t(\kappa)\dot{\varepsilon}_1^p + \frac{1}{g_c} \frac{\sigma_3}{\sigma_1 - \sigma_3} f_c(\kappa)\dot{\varepsilon}_3^p.$$

In particular, in a simple shearing test ($\sigma_1 = \tau = -\sigma_3$, $\sigma_2 = 0$), the rate equation for κ is

$$\dot{\kappa} = \frac{1}{2}\left[\frac{1}{g_t} f_t(\kappa)\dot{\varepsilon}_1^p - \frac{1}{g_c} f_c(\kappa)\dot{\varepsilon}_3^p\right].$$

2.3. *The c–κ relation*

It follows from the discussion in Section 2.1 that the evolution of the cohesion c must be such that $c \to 0$ as $\kappa \to 1$ in any process. In particular, in view of the scaling of c, the rate equation for c, eqn (6), must have the solution $c = f_c(\kappa)$ in a compression test and $c = (f_{c0}/f_{t0}) f_t(\kappa)$ in a tension test.

If, as some investigators, for example Chen (1982), hold, the compressive and tensile stress–strain curves are similar, with $f_c(\kappa)/f_{c0} = f_t(\kappa)/f_{t0}$, then the rate equation (6) may be replaced by the functional relation $c = f_c(\kappa)$. Otherwise, a form must be assumed for $k(\sigma, \kappa, c)$ in eqn (6) which leads to the solutions discussed above. A possible form is

$$k(\sigma, \kappa, c) = c\left[\frac{r(\sigma)}{f_t(\kappa)} f_t'(\kappa) + \frac{1 - r(\sigma)}{f_c(\kappa)} f_c'(\kappa)\right], \tag{13}$$

where $r(\sigma)$ is a weight factor similar to the one discussed previously, and may in fact be likewise assumed to be given by eqn (12).

To show that $c \to 0$ as $\kappa \to 1$ in any process, we note, first, that r will, in general, vary in the course of the process. With the help of eqns (12) and (13), (6) may be written as

$$\mathrm{d} \ln c = r\, \mathrm{d} \ln f_t + (1 - r)\, \mathrm{d} \ln f_c,$$

and, through integration by parts, rewritten as

$$\mathrm{d} \ln c = \mathrm{d}[r \ln f_t + (1 - r)\, \mathrm{d} \ln f_c] + \ln (f_c/f_t)\, \mathrm{d}r.$$

Finally, it can be integrated to yield

$$c = f_{c0}(f_t/f_{t0})^r (f_c/f_{c0})^{1-r} \exp\left[\int \ln (f_c/f_t)\, \mathrm{d}r\right].$$

Since there is no reason to expect the integral $\int_0^{\kappa=1} \ln (f_c/f_t)\, \mathrm{d}r$ to become infinite in any physically realistic process, and since $f_c(1) = f_t(1) = 0$, it follows that $c = 0$ when $\kappa = 1$.

2.4. *The yield surface*

In biaxial tests on concrete and geomaterials it is usually found (Kupfer *et al.*, 1969) that the various critical surfaces in stress space (proportional limit, "discontinuity", "failure") are similar. The same result is *not* found in triaxial compression tests, at least at sufficiently large hydrostatic pressures; under these conditions it is found that the hardening goes on indefinitely. In order words, while the yield surface (however defined) is closed, the failure surface is open in the direction of hydrostatic compression. The so-called *cap* model (DiMaggio and Sandler, 1971) has been used to describe this discontinuity.

The present model is directed toward failure analysis, and therefore no attempt will be made to formulate the yield criterion in the region in which failure does not occur (should this become necessary, the cap model may be resorted to). Equation (2), consequently, is assumed valid only in that part of stress space in which radial loading leads to failure. With $c = f_{c0}$, this equation describes the corresponding part of the initial yield surface, while the failure surface is attained when c reaches its maximum along a given loading path. It is an essential feature of this model that the same function $F(\sigma)$, homogeneous in the first degree in the stress components, describes both.

As was discussed in Section 2.1, the many analytical forms that have been proposed for the failure surface of concrete are not of this nature, except for the Mohr–Coulomb and Drucker–Prager criteria. As a rule, they are quadratic in the octahedral shear stress (or,

equivalently in $\sqrt{J_2}$, where J_2 is the second invariant of the stress deviator) and linear in the mean normal stress (or in I_1, the first invariant of stress); the third invariant enters through the polar angle θ in the deviatoric (π) plane (Chen and Chen, 1975; Ottosen, 1977; Chen, 1982; Podgórski, 1985; Fardis and Chen, 1986). With these forms, the meridians in the $\sigma_1\sigma_2\sigma_3$ space are curved, so that the failure surface tends to a circular cylinder as $I_1 \to -\infty$. If, however, the high-pressure region is excluded, then virtually all available failure data can be fitted quite well into eqn (2), in which $F(\boldsymbol{\sigma})$ has the form

$$F(\boldsymbol{\sigma}) = \frac{1}{1-\alpha}[\sqrt{3J_2} + \alpha I_1 + \beta\langle\sigma_{\max}\rangle - \gamma\langle-\sigma_{\max}\rangle], \tag{14}$$

where α, β and γ are dimensionless constants. This form will be adopted in the present work for the yield surface. Note that when $\sigma_{\max} = 0$, i.e. in biaxial compression, this is just the Drucker–Prager criterion, the only parameter then being α, which can be obtained by comparing the initial equibiaxial and uniaxial compressive yield stresses f_{b0} and f_{c0}:

$$\frac{f_{b0}}{f_{c0}} = \frac{1-\alpha}{1-2\alpha},$$

yielding

$$\alpha = \frac{(f_{b0}/f_{c0}) - 1}{2(f_{b0}/f_{c0}) - 1}. \tag{15}$$

Experimental values of f_{b0}/f_{c0} lie between 1.10 and 1.16, yielding α between 0.08 and 0.12.

Once α is known, β can be determined from f_{c0}/f_{t0}, where f_{t0} is the initial uniaxial tensile yield stress:

$$\frac{f_{c0}}{f_{t0}} = \frac{1+\alpha+\beta}{1-\alpha},$$

or

$$\beta = (1-\alpha)(f_{c0}/f_{t0}) - (1+\alpha).$$

For example, if $\alpha = 0.12$ and $f_{c0} = 10.0f_{t0}$, then $\beta = 7.68$.

The parameter γ appears only in triaxial compression, that is, in stress states with $\sigma_{\max} < 0$. Let TM and CM designate, respectively, the "tensile meridian" ($\sigma_1 > \sigma_2 = \sigma_3$) and the "compressive meridian" ($\sigma_1 = \sigma_2 > \sigma_3$) on the yield surface. On the former,

$$\sigma_{\max} = \tfrac{1}{3}(I_1 + 2\sqrt{3J_2}),$$

and on the latter

$$\sigma_{\max} = \tfrac{1}{3}(I_1 + \sqrt{3J_2}).$$

With $\sigma_{\max} < 0$, the equations of the respective meridians are therefore

$$(2\gamma+3)\sqrt{3J_2} + (\gamma+3\alpha)I_1 = (1-\alpha)f_c \qquad \text{(TM)}$$

and

$$(\gamma+3)\sqrt{3J_2}+(\gamma+3\alpha)I_1=(1-\alpha)f_c: \qquad \text{(CM)}$$

here f_c is the critical stress in uniaxial compression, whether yield stress (for the yield surface) or ultimate stress (for the failure surface). Let us define

$$\rho=\frac{(\sqrt{J_2})_{\text{TM}}}{(\sqrt{J_2})_{\text{CM}}} \quad \text{at a given } I_1;$$

the present model then yields

$$\rho=\frac{\gamma+3}{2\gamma+3}, \tag{16}$$

that is, a constant. The meridians thus described are therefore straight. In spite of the claim of Ottosen (1977) that ρ "increases from 0.5 . . . but remains less than unity", most available experimental failure data are fitted just as well with straight as with curved meridians—that is, with constant values of ρ. Typical values range from about 0.64 (Schickert and Winkler, 1977) and 0.66 (Richart *et al.*, 1982), to about 0.8 (Mills and Zimmerman, 1970). From eqn (16) we obtain

$$\gamma=\frac{3(1-\rho)}{2\rho-1}.$$

A value of $\rho=\frac{2}{3}$ leads to $\gamma=3$.

The form taken by the proposed yield surface on different planes of the stress space is shown in Fig. 3.

2.5. *Flow rule and tangent stiffness*

It is well known that granular materials such as concrete can exhibit a significant volume change when subjected to severe inelastic states. This change in volume, caused by plastic distortion, can be reproduced well by using an adequate plastic potential function G in the definition of the flow rule as given by eqn (4). For the examples analyzed with the present model we have chosen for G the classical Mohr–Coulomb yield function with the angle of dilatancy ψ substituting for the angle of internal friction ϕ (Oñate *et al.*, 1988):

$$G(\sigma,\psi)=\frac{I_1}{3}\sin\psi+\sqrt{J_2}\left(\cos\theta-\frac{\sin\theta\sin\psi}{\sqrt{3}}\right). \tag{17}$$

In the absence of stiffness degradation, the tangent elastic–plastic stiffness operator has the usual form of classical plasticity theory, given in the six-dimensional vector notation for symmetric second-rank tensors by

$$\mathbf{D}^{\text{ep}}=\mathbf{D}-\frac{(\mathbf{Dg})(\mathbf{Df})^{\text{T}}}{H+\mathbf{f}^{\text{T}}\mathbf{Dg}}, \tag{18}$$

where $\mathbf{f}=\partial F/\partial\boldsymbol{\sigma}$, $\mathbf{g}=\partial G/\partial\boldsymbol{\sigma}$ and H is the plastic modulus, given in the case of the present model by $k\mathbf{h}^{\text{T}}\mathbf{g}$. Regardless of whether an associated flow rule ($\mathbf{g}=\mathbf{f}$) is used or not, eqn (18) requires the values of the normal vector $\mathbf{f}$ to the yield surface. However, the yield surface presented in Section 2.4 is not smooth, and a decision must be made as to the value of $\mathbf{f}$ at the singular points.

The singular points of the yield surface are the following: (a) those where the maximum normal stress changes direction, comprising the compression meridians; (b) those where the maximum normal stress changes sign, belonging to the intersection of the yield surface with the three quarter-planes that bound the triaxial compression octant, namely (i) $\sigma_1=0$, $\sigma_2<0$, $\sigma_3<0$, (ii) $\sigma_1<0$, $\sigma_2=0$, $\sigma_3<0$, (iii) $\sigma_1<0$, $\sigma_2<0$, $\sigma_3=0$.

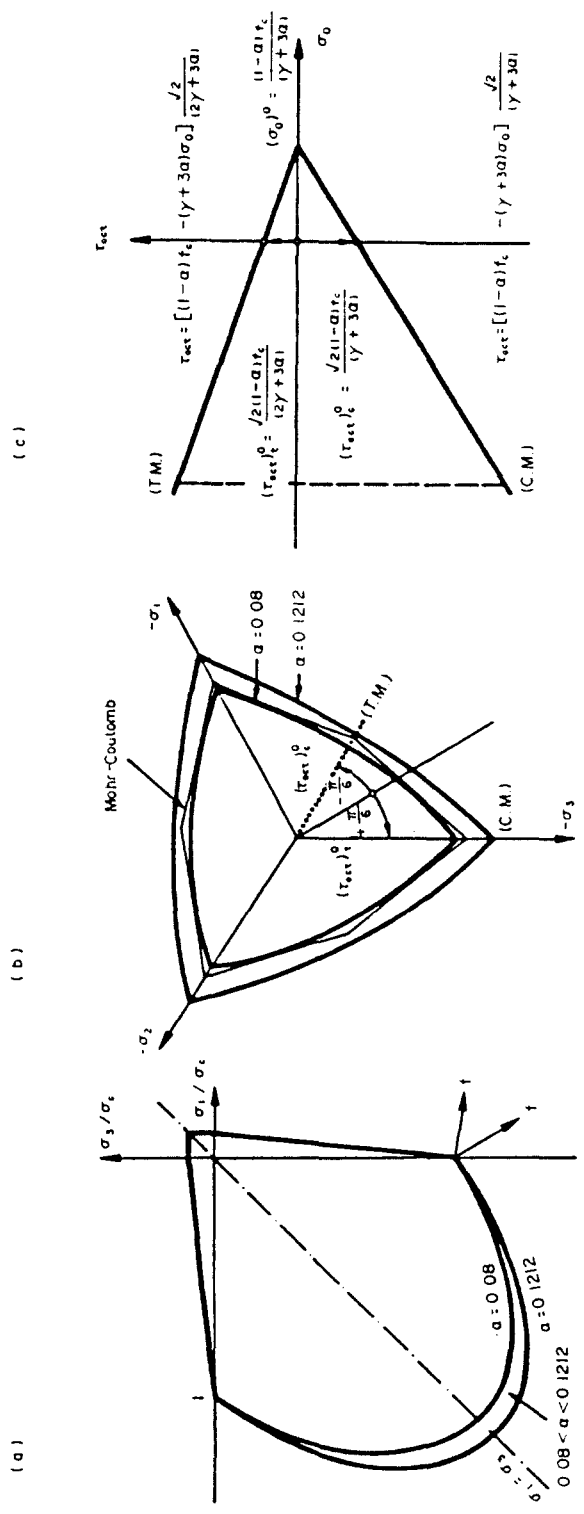

Fig. 3. Proposed yield surface: (a) $(\sigma_1-\sigma_3;\ \sigma_2=0)$ plane; (b) octahedral plane; (c) meridian plane.

The compression meridian, say $\sigma_1 = \sigma_2 > \sigma_3$, includes cases of axial symmetry, in which, by virtue of said symmetry, one must have $f_1 = f_2$. It is not unreasonable to extend this rule to all cases corresponding to compression meridians—that is, to place **f** exactly midway between the bounding normals.

The other set of singular points is of great importance because it includes biaxial (and, as a special case, uniaxial) compression. Suppose that $\sigma_1 > \sigma_2 \geqslant \sigma_3$. Differentiating the right-hand side of (14) with respect to σ_1 yields

$$f_1 = \frac{1}{1-\alpha}\left(\frac{3s_1}{\sqrt{3J_2}} + \alpha + \delta\right),$$

where $\delta = \beta$ if $\sigma_1 > 0$, $\delta = \gamma$ if $\sigma_1 < 0$, and δ is indeterminate in the range between β and γ if $\sigma_1 = 0$. In this case there is no symmetry argument to dictate a choice of δ, and recourse must be made to empirical information.

Andanaes *et al.* (1977) report that concrete under biaxial stress apparently does not exhibit normality of the plastic strain-rate vector to the yield surface, although the results are not altogether clear because the authors do not spell out how they define elastic strain—that is, whether it is defined by the initial modulus or (as it should be) by the current (degraded) secant modulus. If it is the former, then a correction would bring the results closer to normality. Even without this correction, however, normality is fairly closely approached at uniaxial compression *in the limit from the biaxial compression quadrant*. This indicates that, if an associated flow rule were used with the present yield surface, then at the singular points corresponding to $\sigma_{\max} = 0$, δ would have the value γ. This result will be adopted as a working rule for the definition of **f** at the singular points belonging to category (b).

Uniaxial compression is represented by a point that is the intersection of the just-discussed singularity locus with a compression meridian. If $\sigma_1 = \sigma_2 = 0$ and $\sigma_3 < 0$, the rule we have adopted yields

$$f_1 = f_2 = \frac{1}{1-\alpha}\left(\frac{1}{2} + \alpha + \gamma\right),$$

$$f_3 = \frac{1}{1-\alpha}(-1+\alpha) = -1.$$

With an associated flow rule, this result gives the following value of the ratio of the transverse to the axial *total* strain rates:

$$-\frac{\dot{\varepsilon}_1}{\dot{\varepsilon}_3} = -\frac{\dot{\varepsilon}_2}{\dot{\varepsilon}_3} = \frac{1+2\alpha+2\gamma}{2(1-\alpha)}\left(1-\frac{E_t}{E}\right)+\nu\frac{E_t}{E},$$

where E is the elastic Young's modulus, ν is the elastic Poisson's ratio and E_t is the current tangent modulus.

3. THE EFFECT OF STIFFNESS DEGRADATION

3.1. *General considerations*

In the presence of stiffness degradation, i.e. when the elastic stiffness **D** varies in the course of deformation, the preceding results must be modified, in particular with regard to the formulation of an associated flow rule.

It will be assumed that stiffness degradation can be described through the dependence of the stiffness **D** on two sets of scalar-valued internal variables, to be called the *elastic* and *plastic* degradation variables, and to be denoted $d_1, d_2, \ldots$ and $\delta_1, \delta_2, \ldots$, respectively. The former are similar to the *damage variables* such as those considered by Simo and Ju

(1987) and others, in that their variation is associated with the total deformation, but without the necessity of a *damage criterion*. Their evolution will be assumed to be governed by rate equations of the form

$$\dot{d}_i = \phi_i \langle \mathbf{k}_i^{\mathrm{T}} \dot{\boldsymbol{\varepsilon}} \rangle, \tag{19}$$

where $\mathbf{k}_i$ is a vector in stress space denoting the direction of what may be called *degradation loading* associated with the variable d_i, and ϕ_i is a positive scalar factor; the ϕ_i and $\mathbf{k}_i$ are functions of $\boldsymbol{\sigma}$ and the d_i, and the ϕ *may* incorporate a damage threshold in the sense that they may vanish inside some surface in the space of the state variables.

The plastic degradation variables δ_j are those associated with plastic deformation, and constitute a special case of the damage variables introduced by Chaboche (1977), in that they are governed by the rate equations

$$\dot{\delta}_j = \dot{\lambda} \mu_j, \tag{20}$$

where $\dot{\lambda}$ is the plastic loading factor in the flow rule (4). With the further choice $\mu_j = \mathbf{l}_j^{\mathrm{T}} \mathbf{g}$, these rate equations become

$$\dot{\delta}_j = \mathbf{l}_j^{\mathrm{T}} \dot{\boldsymbol{\varepsilon}}^{\mathrm{p}}, \tag{21}$$

where the $\mathbf{l}_j$ are likewise vectors in stress space.

A distinction between the degradation variables used here and the damage variables that appear in continuum damage mechanics is that we do not invoke the concept of *effective stress* introduced by Kachanov (1958) and developed by Rabotnov (1969) and others, such as Martin and Leckie (1972) and Hayhurst and Leckie (1973). According to this concept, the equations governing the behavior of the damaged material are obtained from those of the undamaged material by replacing the true stress $\boldsymbol{\sigma}$ by the effective stress $\boldsymbol{\sigma}/(1-d)$, where d is the damage variable; therefore the stiffness $\mathbf{D}$ is replaced by $(1-d)\mathbf{D}$. However, while the notion of effective stress may be appropriate in metal plasticity and creep in view of its microphysical basis, it is less so in the case of concrete and geomaterials. It will consequently be assumed, at least to begin with, that $\mathbf{D}$ depends on the degradation variables in a general way, so that

$$\boldsymbol{\sigma} = \mathbf{D}(d_1, \ldots ; \delta_1, \ldots)(\boldsymbol{\varepsilon} - \boldsymbol{\varepsilon}^{\mathrm{p}}).$$

It follows by differentiation with respect to time that

$$\dot{\boldsymbol{\sigma}} = \dot{\mathbf{D}} \mathbf{D}^{-1} \boldsymbol{\sigma} + \mathbf{D}(\dot{\boldsymbol{\varepsilon}} - \dot{\boldsymbol{\varepsilon}}^{\mathrm{p}}).$$

Now, from the chain rule and eqns (19) and (21),

$$\dot{\mathbf{D}} = \sum_i \phi_i \partial \mathbf{D} / \partial d_i \langle \mathbf{k}_i^{\mathrm{T}} \dot{\boldsymbol{\varepsilon}} \rangle + \sum_j \partial \mathbf{D} / \partial \delta_j \mathbf{l}_j^{\mathrm{T}} \dot{\boldsymbol{\varepsilon}}^{\mathrm{p}}.$$

We define the operator $\mathbf{C}_{\mathrm{e}}$ by

$$\mathbf{C}_{\mathrm{e}} \dot{\boldsymbol{\varepsilon}} = \mathbf{D} \dot{\boldsymbol{\varepsilon}} + \sum_i \phi_i \partial \mathbf{D} / \partial d_i \mathbf{D}^{-1} \boldsymbol{\sigma} \langle \mathbf{k}_i^{\mathrm{T}} \dot{\boldsymbol{\varepsilon}} \rangle ; \tag{22}$$

note that C_{e} is a *nonlinear* operator in that it depends on the direction of $\dot{\boldsymbol{\varepsilon}}$.

We also define the linear operator

$$\mathbf{C}_p = \mathbf{D} - \sum_j \hat{c}\mathbf{D}/\partial\delta_j \mathbf{D}^{-1}\boldsymbol{\sigma}\mathbf{l}_j^{\mathrm{T}}. \tag{23}$$

From the definitions (22) and (23) it follows that

$$\dot{\boldsymbol{\sigma}} = \mathbf{C}_e\dot{\boldsymbol{\varepsilon}} - \mathbf{C}_p\dot{\boldsymbol{\varepsilon}}^{\mathrm{p}}. \tag{24}$$

Let the yield criterion be given, as before, by eqn (2). Note that we are omitting any dependence of the yield criterion on the degradation variables, in contrast to the *continuum damage mechanics* model based on the aforementioned notion of effective stress, which necessarily brings the damage variable into the yield criterion. As we said above, this model has a physical basis for metals, but in the case of concrete and geomaterials the theory of plasticity is at best an approximate mathematical model of behavior, and its usefulness would be impaired by complications.

The consistency condition

$$\mathbf{f}^{\mathrm{T}}\dot{\boldsymbol{\sigma}} = \dot{c},$$

where $\mathbf{f} = \hat{c}F/\hat{c}\boldsymbol{\sigma}$, combined with eqns (5), (6), (9), and (24), yields

$$\mathbf{f}^{\mathrm{T}}\mathbf{C}_e\dot{\boldsymbol{\varepsilon}} = (H + \mathbf{f}^{\mathrm{T}}\mathbf{C}_p\mathbf{g})\dot{\lambda},$$

where

$$H = k\mathbf{h}^{\mathrm{T}}\mathbf{g} \tag{25}$$

is the plastic modulus, whenever $\dot{\lambda} > 0$. Stability under strain control implies that

$$H + \mathbf{f}^{\mathrm{T}}\mathbf{C}_p\mathbf{g} > 0,$$

and this condition will be assumed to be met. Consequently

$$\dot{\lambda} = \frac{\langle \mathbf{f}^{\mathrm{T}}\mathbf{C}_e\dot{\boldsymbol{\varepsilon}} \rangle}{H + \mathbf{f}^{\mathrm{T}}\mathbf{C}_p\mathbf{g}}, \tag{26}$$

and therefore the elastic–plastic tangent stiffness operator is defined by

$$\dot{\boldsymbol{\sigma}} = \mathbf{C}_e\dot{\boldsymbol{\varepsilon}} - \mathbf{C}_p\mathbf{g}\frac{\langle \mathbf{f}^{\mathrm{T}}\mathbf{C}_e\dot{\boldsymbol{\varepsilon}} \rangle}{H + \mathbf{f}^{\mathrm{T}}\mathbf{C}_p\mathbf{g}} \tag{27}$$

in place of eqn (18). The tangent stiffness, as a piecewise linear operator, is symmetric if $\mathbf{C}_e$ is symmetric *and* if $\mathbf{C}_p\mathbf{g}$ is proportional to $\mathbf{C}_e^{\mathrm{T}}\mathbf{f}$. The symmetry of $\mathbf{C}_e$ will be examined in the next section, while in the following one it will be shown that the aforementioned proportionality is an appropriate form of the associated flow rule in the presence of stiffness degradation.

3.2. *Elastic degradation*

The simplest hypothesis of elastic degradation is based on a single variable d (Kachanov, 1958), such that

$$\mathbf{D} = (1 - d)\mathbf{D}_0, \tag{28}$$

where $\mathbf{D}_0$ is the initial stiffness. For an isotropic solid, this hypothesis implies a constant Poisson's ratio, which several investigators, e.g. Kupfer *et al.* (1969), have reported for concrete up to a stress level that approximately coincides with the onset of major cracking

(typically some 75–80% of the ultimate stress) and that therefore may be reasonably taken as representing the yield stress. Equation (28) leads to the operator $\mathbf{C}_e$ given by

$$\mathbf{C}_e\dot{\boldsymbol{\varepsilon}} = \mathbf{D}\dot{\boldsymbol{\varepsilon}} - \frac{\phi}{1-d}\boldsymbol{\sigma}\langle \mathbf{k}^{\mathrm{T}}\dot{\boldsymbol{\varepsilon}}\rangle. \tag{29}$$

Thus C_e is symmetric if and only if $\mathbf{k}$ is proportional (or equal, with no loss of generality, since any proportionality factor can be absorbed in ϕ) to $\boldsymbol{\sigma}$. In other words, elastic stiffness degradation is associated with an increase in the total deformation work. Note that, in the elastic range, $\boldsymbol{\sigma}^{\mathrm{T}}\dot{\boldsymbol{\varepsilon}} = (1-d)\dot{W}_0$, where $2W_0 = \boldsymbol{\varepsilon}^{\mathrm{T}}\mathbf{D}\boldsymbol{\varepsilon}$, is the square of the *undamaged energy norm* of the strain (Simo and Ju, 1987).

However, the majority of investigators of the multiaxial behavior of concrete (see Cedolin *et al.*, 1977 for a survey; also Andanaes *et al.*, 1977) have found degradation behavior that is not described by eqn (28). Instead, they have found that the bulk modulus depends primarily on the volume strain, and the shear modulus on the octahedral shear strain. In the elastic range, this dependence is equivalent to one in which the bulk and shear moduli are determined respectively by the volume work and distortional work, and can be described by assuming, in place of eqn (28) that

$$K = (1-d_1)K_0, \quad G = (1-d_2)G_0, \tag{30}$$

where K (G) and K_0 (G_0) denote respectively the current and initial values of the secant bulk (shear) modulus.

The 6×6 stiffness matrix of an isotropic solid can be written in the form

$$\mathbf{D} = K\mathbf{1}\mathbf{1}^{\mathrm{T}} + G\mathbf{U}\mathbf{dev},$$

where $\mathbf{1} = (1,1,1,0,0,0)$, $\mathbf{dev} = \mathbf{I} - \frac{1}{3}\mathbf{1}\mathbf{1}^{\mathrm{T}}$ ($\mathbf{I}$ being the 6×6 identity matrix), and

$$\mathbf{U} = \begin{bmatrix} 2 & 0 & 0 & 0 & 0 & 0 \\ 0 & 2 & 0 & 0 & 0 & 0 \\ 0 & 0 & 2 & 0 & 0 & 0 \\ 0 & 0 & 0 & 1 & 0 & 0 \\ 0 & 0 & 0 & 0 & 1 & 0 \\ 0 & 0 & 0 & 0 & 0 & 1 \end{bmatrix}.$$

Thus

$$\mathbf{D}^{-1} = \frac{1}{9K}\mathbf{1}\mathbf{1}^{\mathrm{T}} + \frac{1}{G}\mathbf{U}^{-1}\mathbf{dev},$$

where

$$\mathbf{U}^{-1} = \begin{bmatrix} \frac{1}{2} & 0 & 0 & 0 & 0 & 0 \\ 0 & \frac{1}{2} & 0 & 0 & 0 & 0 \\ 0 & 0 & \frac{1}{2} & 0 & 0 & 0 \\ 0 & 0 & 0 & 1 & 0 & 0 \\ 0 & 0 & 0 & 0 & 1 & 0 \\ 0 & 0 & 0 & 0 & 0 & 1 \end{bmatrix}$$

and therefore, since $\mathbf{U}\,\mathbf{dev}\,\mathbf{U}^{-1}\mathbf{dev} = \mathbf{dev}$,

$$\mathbf{C}_e\dot{\boldsymbol{\varepsilon}} = \mathbf{D}\dot{\boldsymbol{\varepsilon}} - \frac{\phi_1}{1-d_1}\sigma_0\mathbf{1}\langle\mathbf{k}_1^T\dot{\boldsymbol{\varepsilon}}\rangle - \frac{\phi_2}{1-d_2}\mathbf{s}\langle\mathbf{k}_2^T\dot{\boldsymbol{\varepsilon}}\rangle,$$

where $\sigma_0 = \frac{1}{3}\mathbf{1}^T\boldsymbol{\sigma}$ is the mean normal stress, and $\mathbf{s} = \mathbf{dev}\boldsymbol{\sigma}$ is the stress deviator. Consequently $\mathbf{C}_e$ is symmetric in all processes if and only if $\mathbf{k}_1 = \sigma_0\mathbf{1}$ and $\mathbf{k}_2 = \mathbf{s}$—that is, if the bulk and shear stiffnesses are associated, respectively, with an increase in the volume and distortional deformation work.

Let us consider, for example, an exponential dependence of the moduli on the corresponding strain, i.e. a dependence given by

$$K = K_0 e^{-a_1\varepsilon_v}, \quad G = G_0 e^{-a_2\gamma_{oct}},$$

where a_1 and a_2 are constants, and $\varepsilon_v = \mathbf{1}^T\boldsymbol{\varepsilon}$ and $\gamma_{oct} = 2\sqrt{\boldsymbol{\varepsilon}^T\mathbf{U}\boldsymbol{\varepsilon}/6}$ are the volume strain and the octahedral shear strain, respectively. It can be shown that these functions can be obtained, in monotonic radial loading, from the following forms of ϕ_1 and ϕ_2:

$$\phi_1 = \frac{a_1(1-d_1)}{|\sigma_0|}, \quad \phi_2 = \sqrt{\frac{2}{3}}\frac{a_2(1-d_2)}{\sqrt{J_2}}.$$

3.3. *The associated flow rule*

It is well known in classical plasticity theory that what is generally known as the associated flow rule—that is, the normality of the plastic strain-rate tensor to the yield surface in stress space—is equivalent to the axiom of *maximum plastic dissipation* (MPD) when the elastic stiffness is constant, or, more generally, when the free energy (at a given temperature) may be decomposed as

$$\psi = \psi_e(\boldsymbol{\varepsilon} - \boldsymbol{\varepsilon}^p) + \psi_p(\alpha_1, \alpha_2, \ldots),$$

where the α_i are the *plastic* internal variables i.e. variables whose rates vanish whenever $\dot{\boldsymbol{\varepsilon}}^p = 0$. Such consequences of the associated flow rule as uniqueness of solutions to boundary-value problems and the theorems of limit analysis flow largely from the MPD axiom, which has also been helpful in clarifying the form taken by the associated flow rule in large-deformation plasticity (Lubliner, 1984, 1986).

In its most general form, the MPD axiom may be expressed as follows. Let the free energy be written as $\psi(\boldsymbol{\varepsilon}^e, \alpha_1, \ldots, \beta_1, \ldots)$, where $\boldsymbol{\varepsilon}^e = \boldsymbol{\varepsilon} - \boldsymbol{\varepsilon}^p$ is the elastic strain, the α_i are the plastic internal variables as above and the β_j are any other internal variables. The total dissipation is

$$D = \boldsymbol{\sigma}^T\dot{\boldsymbol{\varepsilon}} - \dot{\psi}.$$

Since $\boldsymbol{\sigma} = \partial\psi/\partial\boldsymbol{\varepsilon}^e$, the dissipation may be decomposed as

$$D = D_d + D_p,$$

where

$$D_d = -\sum_j \frac{\partial\psi}{\partial\beta_j}\dot{\beta}_j$$

and

$$D_p = \boldsymbol{\sigma}^T \dot{\boldsymbol{\varepsilon}}^p - \sum_i \frac{\partial \psi}{\partial \alpha_i} \dot{\alpha}_i.$$

The latter is the plastic dissipation, a function of $\boldsymbol{\varepsilon} - \boldsymbol{\varepsilon}^p, \alpha_1, \ldots, \beta_1, \ldots ; \dot{\boldsymbol{\varepsilon}}^p, \dot{\alpha}_1, \ldots$. The MPD axiom assumes that

$$D_p(\boldsymbol{\varepsilon} - \boldsymbol{\varepsilon}^p, \alpha_1, \ldots, \beta_1, \ldots ; \dot{\boldsymbol{\varepsilon}}^p, \dot{\alpha}_1, \ldots) \geqslant D_p(\boldsymbol{\varepsilon}^* - \boldsymbol{\varepsilon}^p, \alpha_1, \ldots, \beta_1, \ldots ; \dot{\boldsymbol{\varepsilon}}^p, \dot{\alpha}_1, \ldots) \tag{31}$$

if $\boldsymbol{\varepsilon}^*$ is a state of strain that can be attained from $\boldsymbol{\varepsilon}$ by means of an elastic process, i.e. one with no change in $\boldsymbol{\varepsilon}^p$, the α_i or the β_j. In simple cases inequality (31) reduces to the well-known form

$$\boldsymbol{\sigma}^T \dot{\boldsymbol{\varepsilon}}^p \geqslant \boldsymbol{\sigma}^{*T} \dot{\boldsymbol{\varepsilon}}^p.$$

With D_p a differentiable function of $\boldsymbol{\varepsilon} - \boldsymbol{\varepsilon}^p$, inequality (31) may also be expressed in the local form

$$\dot{\boldsymbol{\varepsilon}}^T \partial D_p / \partial \boldsymbol{\varepsilon} \geqslant 0. \tag{32}$$

For an elastic-plastic solid exhibiting linear elasticity with degradation as described in Section 3.1, the free energy may be written as

$$\psi = \tfrac{1}{2}(\boldsymbol{\varepsilon} - \boldsymbol{\varepsilon}^p)^T \mathbf{D}(\boldsymbol{\varepsilon} - \boldsymbol{\varepsilon}^p) + \psi_p(\alpha_1, \ldots),$$

where $\mathbf{D}$ depends on the d_i and δ_i, as before. Note that the δ_i are included among the α_i. The plastic dissipation is, accordingly,

$$D_p = (\boldsymbol{\varepsilon} - \boldsymbol{\varepsilon}^p)^T \left[\mathbf{D} - \frac{1}{2} \sum_j \partial \mathbf{D} / \partial \delta_j (\boldsymbol{\varepsilon} - \boldsymbol{\varepsilon}^p) \mathbf{l}_j^T \right] \dot{\boldsymbol{\varepsilon}}^p - \dot{\psi}_p,$$

and the local form of the MPD axiom, inequality (32), becomes

$$\dot{\boldsymbol{\varepsilon}}^T \left[\mathbf{D} - \sum_j \partial \mathbf{D} / \partial \delta_j (\boldsymbol{\varepsilon} - \boldsymbol{\varepsilon}^p) \mathbf{l}_j^T \right] \dot{\boldsymbol{\varepsilon}}^p \geqslant 0,$$

or, in view of eqn (23),

$$\dot{\boldsymbol{\varepsilon}}^T \mathbf{C}_p \dot{\boldsymbol{\varepsilon}}^p \geqslant 0.$$

The flow rule (4) implies that

$$\dot{\boldsymbol{\varepsilon}}^T \mathbf{C}_p \mathbf{g} \geqslant 0 \tag{33}$$

whenever $\dot{\lambda} > 0$, that is, whenever

$$\dot{\boldsymbol{\varepsilon}}^T \mathbf{C}_e^T \mathbf{f} \geqslant 0, \tag{34}$$

in view of eqn (26). The simultaneous satisfaction of inequalities (33) and (34) requires that $\mathbf{C}_p \mathbf{g}$ be proportional to or, with no loss of generality, equal to $\mathbf{C}_e^T \mathbf{f}$:

$$\mathbf{C}_p \mathbf{g} = \mathbf{C}_e \mathbf{f}. \tag{35}$$

In a solid with elastic and plastic stiffness degradation as defined here, then, the flow rule

(4) may be regarded as associated if $\mathbf{g}$ obeys eqn (35). In the absence of degradation, $\mathbf{C}_e = \mathbf{C}_p = \mathbf{D}$ and therefore the classical form $\mathbf{g} = \mathbf{f}$ is recovered.

If eqn (35) holds, the tangent elastic–plastic stiffness is defined by

$$\dot{\sigma} = \mathbf{C}_e\dot{\varepsilon} = \mathbf{C}_e\dot{\varepsilon} - \mathbf{C}_e^T\mathbf{f}\frac{\langle \mathbf{f}^T\mathbf{C}_e\dot{\varepsilon}\rangle}{H + \mathbf{f}^T\mathbf{C}_e^T\mathbf{f}}. \tag{36}$$

It thus differs from the classical form only in that the constant elastic stiffness $\mathbf{D}$ is replaced by $\mathbf{C}_e$.

3.4. *Plastic degradation—an example*

A simple model of plastic degradation that may be appropriate for concrete is based on the assumption that plastic degradation occurs only in the softening range, and that the stiffness is then proportional to the cohesion—that is, there is only one plastic degradation variable $\delta = \delta_1$, with the current stiffness given by

$$\mathbf{D} = (1-\delta)\mathbf{D}_e(d_1, \ldots),$$

and with δ governed by the rate equation

$$\dot{\delta} = \frac{1-\delta}{c}\langle -\dot{c}\rangle,$$

the initial value δ being zero, so that, in the softening range ($\dot{c} < 0$),

$$\delta = 1 - \frac{c}{c_{\max}}.$$

The vector $\mathbf{l} = \mathbf{l}_1$ appearing in eqn (21) is accordingly given by

$$\mathbf{l} = \frac{1-\delta}{c}\langle -k\rangle\mathbf{h}^T,$$

the quantities $\mathbf{h}$ and k being those of eqns (5) and (6). Thus

$$\mathbf{C}_p = \mathbf{D} + \frac{\langle -k\rangle}{c}\boldsymbol{\sigma}\mathbf{h}^T.$$

Equation (35) may now be solved for $\mathbf{g}$:

$$\mathbf{g} = \mathbf{D}^{-1}\left[\mathbf{C}_e^T\mathbf{f} - \frac{\langle -k\rangle\mathbf{h}^T\mathbf{D}^{-1}\mathbf{C}_e^T\mathbf{f}}{c + \langle -k\rangle\mathbf{h}^T\mathbf{D}^{-1}\boldsymbol{\sigma}}\boldsymbol{\sigma}\right]. \tag{37}$$

The plastic modulus H as defined by eqn (25) is given by

$$H = \frac{ck\mathbf{h}^T\mathbf{D}^{-1}\mathbf{C}_e^T\mathbf{f}}{c + \langle -k\rangle\mathbf{h}^T\mathbf{D}^{-1}\boldsymbol{\sigma}}. \tag{38}$$

4. NUMERICAL EXPERIMENTATION

The constitutive model presented has been implemented in a standard finite element program for non-linear analysis of structures and applied to evaluate the numerical response of several specimens for which experimental results are known. Before entering in the

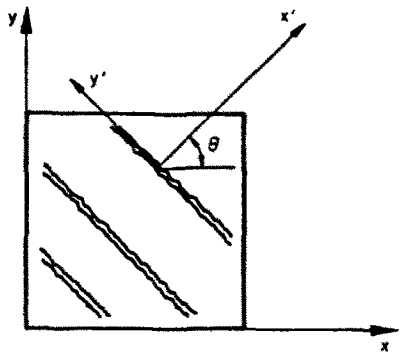

Fig. 4. Direction of cracking.

discussion of the examples analyzed, some general considerations on the definition and representation of cracking have to be mentioned.

Cracking is the most important external manifestation of damage in a concrete structure. In order to obtain a graphic representation of this kind of damage, some parameters are evaluated at each integration point *a posteriori*, once convergence of the non-linear solution has been reached. This can be interpreted as a postprocessing of the results in which conditions for onset of cracking, *crack directions*, *plastic strains* (as a measure at the opening of the cracks), *energy dissipation* and *shear-retention factor* are computed by means of the following procedure:

(a) Cracking initiates at a point when the plastic-damage variable κ is greater than zero, and the maximum principal plastic strain is positive. The direction of cracking is assumed to be orthogonal to that of the maximum principal plastic strain at the damaged point. Other criteria for defining onset and directions of cracking as the *localization condition* based on the acoustic tensor (Willam and Sobh, 1987), or *maximum energy release* (Bažant, 1986), are also possible.

(b) The vector of plastic strains along the directions of the crack, $\mathbf{e}^{cr}$, can be obtained in terms of the plastic strains $\boldsymbol{\varepsilon}^{p}$ expressed in global Cartesian axes as:

$$\mathbf{e}^{cr} = \begin{Bmatrix} \varepsilon_x^{cr} \\ \gamma_{xy}^{cr} \end{Bmatrix} = \begin{bmatrix} \cos^2 2\theta & \sin^2 \theta & \tfrac{1}{2}\sin 2\theta \\ -\sin 2\theta & \sin 2\theta & \cos 2\theta \end{bmatrix} \begin{Bmatrix} \varepsilon_x^{cr} \\ \varepsilon_y^{cr} \\ \gamma_{xy}^{cr} \end{Bmatrix}, \tag{39}$$

where θ is the angle which the direction of the maximum principal strain forms with the global x-axis (see Fig. 4). The vector $\mathbf{e}^{cr}$ is used as a measure of the opening and sliding of the crack.

(c) The energy dissipated in the structure due to cracking in a load increment is obtained as

$$\Delta W^{p} = \int_{V} \boldsymbol{\sigma}^{T} \Delta \boldsymbol{\varepsilon}^{p} \, dV, \tag{40}$$

where V is the volume of the structure.

(d) The shear retention factor (Rots *et al.*, 1985), at a crack is obtained as $\beta = \tau_{x'y'}/\tau^{e}_{x'y'}$, where $\tau_{x'y'}$ is the shear stress parallel to the direction of the crack and $\tau^{e}_{x'y'}$ is the value obtained from a linear-elastic analysis as $\tau_{x'y'} = G_o \gamma_{x'y'}$, where G_o is the elastic shear modulus.

4.1. *Example* 1: *biaxial compression test*

The first example presented is the application of the model to the well known biaxial compression test of Kupfer *et al.* (1969). The example consists of the study of the behavior

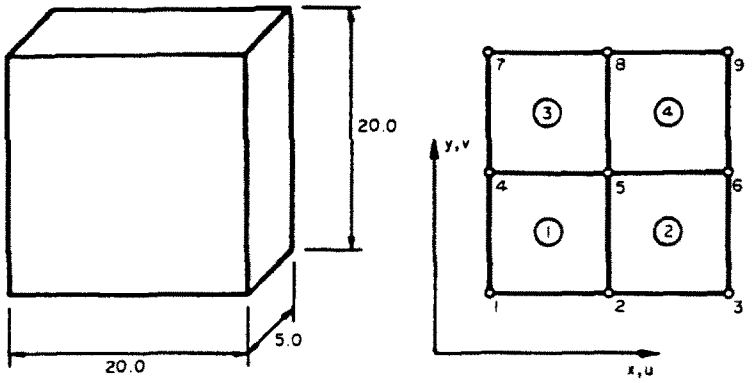

$E_0 = 395000.00$ kg cm^{-2}
$\nu_0 = 0.24$
$f_{c0} = -229.00$ kg cm^{-2}
$f_{c,peak} = -328.00$ kg cm^{-2}
$f_{t0} = 22.90$ kg cm^{-2}
$\alpha = 0.12 - \frac{f_{b0}}{f_{c0}} = 1.16$
$\gamma = 3.0$
$G_f = 0.16$ kg cm^{-1}
$G_c = 16.00$ kg cm^{-1}
Associated flow: Yield and potential function, proposed
Non-associated flow: Yield function proposed; Potential function, Mohr-Coulomb with $\phi = \psi = 15°$

Fig. 5. Biaxial compression test. Relevant material parameters and finite-element mesh.

of a concrete specimen of $20 \times 20 \times 5$ cm (see Fig. 5) subjected to different loading conditions – pure compression, double symmetric compression and double non-symmetric compression.

The geometry of the test, material properties data and the finite element mesh of four standard 4-noded rectangular elements used for the analysis are shown in Fig. 5. In all cases an initial stress approach, which circumvents the problem of non-symmetry of the stiffness matrix due to non-associated plasticity, has been used. Also, displacements have been controlled using a standard spherical path technique (Crisfield, 1981).

4.1.1. *Pure compression:* $\sigma_{22}/\sigma_{11} = -1/0$ *and* $\sigma_{33} = 0$. In Fig. 6(a) numerical results obtained with our model for associated and non-associated plasticity have been plotted. Excellent agreement of numerical results for the σ_{22}–ε_{22} curve with experimental test, also plotted in the Fig. 6, is obtained for both cases. Good agreement between experimental and numerical results is also obtained for the σ_{22}–ε_{11} curve. However, associated plasticity seems to match experimental results better after the stress peak in this case.

In Fig. 6(b), numerical results obtained by different researchers for the same problem are shown for comparison. Finally, in Fig. 7, the crack directions obtained at total failure in the Gauss points are shown.

4.1.2. *Double symmetric compression:* $\sigma_{22}/\sigma_{11} = -1/-1$ *and* $\sigma_{33} = 0$. Numerical results for the σ_{22}–ε_{22} (or σ_{11}–ε_{11}) curve as shown in Fig. 8(a). Good agreement with available experimental data (Kupfer *et al.*, 1969), is obtained for both associated and non-associated plasticity. However, some perturbations of numerical results towards the end of the test can be observed. These are due to the well-known *locking effect* in 4-noded rectangular elements working under incompressibility conditions, as is the case in the example analyzed when plastic strains develop. This spurious effect can be eliminated by using reduced integration and other numerical techniques (Crook and Hinton, 1987). Results obtained by different researchers for the same problem have been plotted in Fig. 8(b) for comparison.

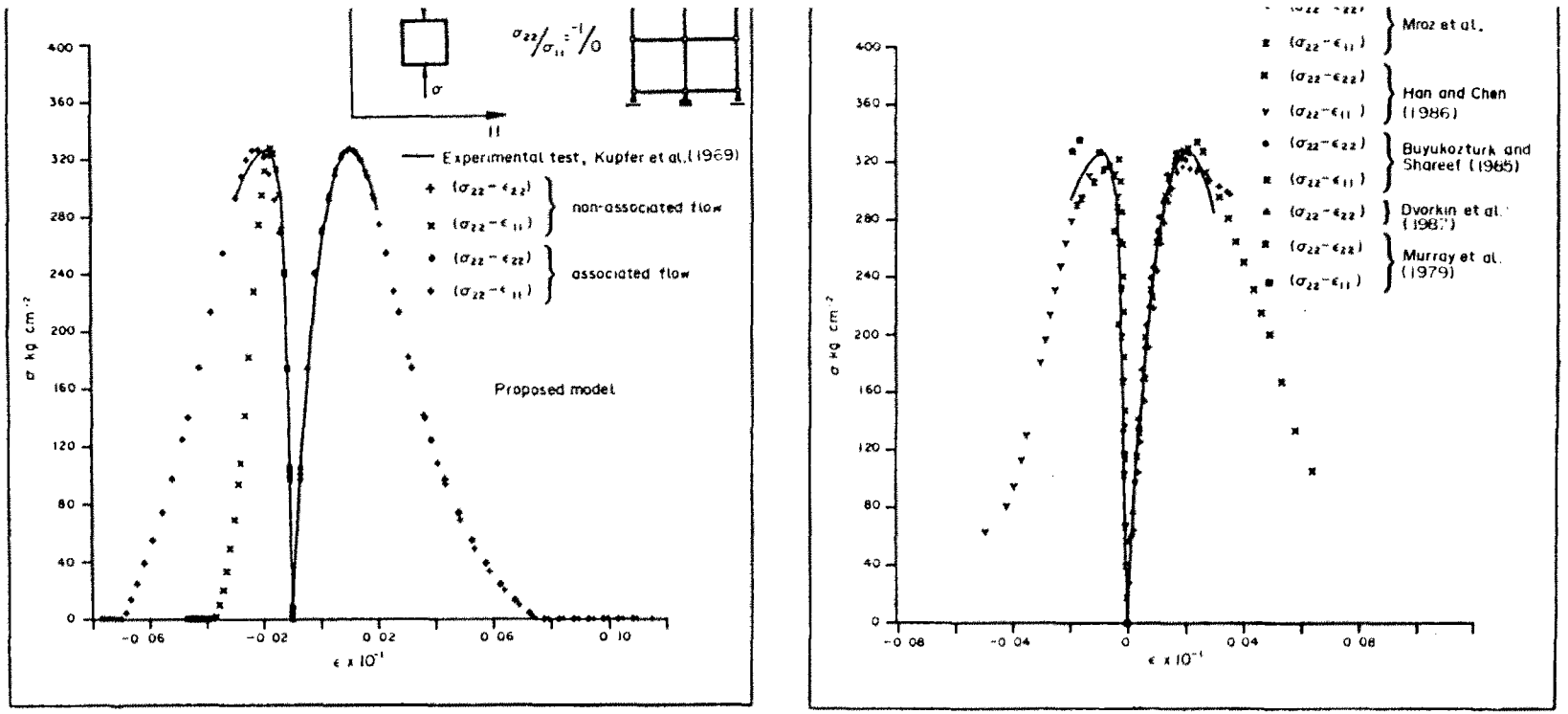

Fig. 6. Biaxial compression test. Compared stress-strain results for pure symmetric compression.

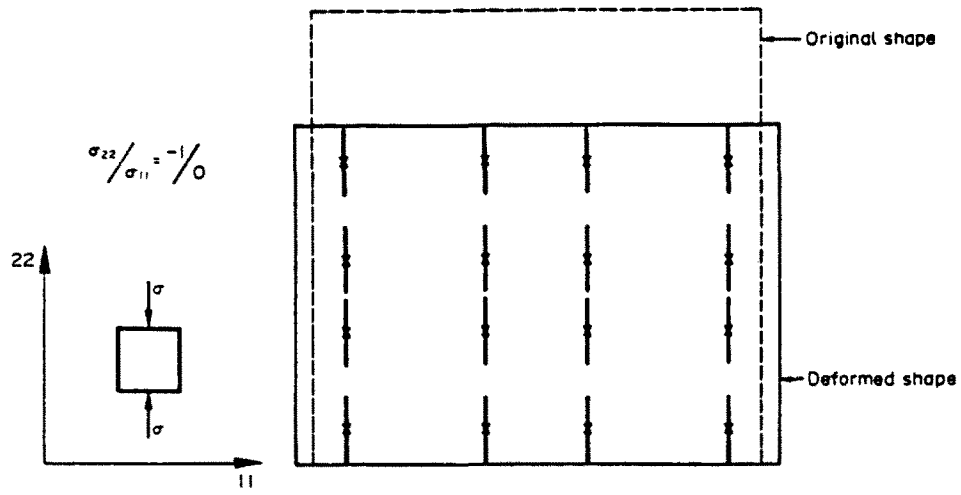

Fig. 7. Biaxial compression test. Distribution of cracking for pure symmetric compression.

4.1.3. *Double non-symmetric compression*: σ_{22}–$\sigma_{11} = -1/-0.52$ *and* $\sigma_{33} = 0$. Numerical results obtained for the σ_{22}–ε_{22} and σ_{22}–ε_{11} curves are shown in Fig. 9(a). Results agree reasonably well with those reported by Kupfer *et al.* (1969), with errors of 3% and 15% in the peak stress and the corresponding strains, respectively, for the σ_{22}–ε_{22} curve for both associated and non-associated plasticity analysis. The use of non-associated plasticity seems to be more important to match experimental results for the σ_{22}–ε_{11} curve, although the peak response is not very precisely reproduced in this case. The difficulties of analyzing this problem are evidenced in the reproduction of the numerical results obtained by various researchers shown in Fig. 9(b).

4.2. *Example* 2: *analysis of a notched beam mixed fracture mode*

This example is a reproduction of the experimental test performed by Arrea and Ingraffea (1981). The geometry of the notched beam, material data and loading conditions used to induce a mixed fracture mode (modes I and II) are shown in Fig. 10. As it can be seen in the figure, the steel beam, used to transmit the loads to the concrete beam, has also been considered in the analysis (assuming linear behavior) in order to take its rigidity into account. The numerical analysis was performed using eight-noded two dimensional finite elements, and the mesh used is shown in Fig. 10(a). The *crack mouth sliding displacement* (CMSD) at the notch tip (see Fig. 10(b)) was controlled using a spherical path technique (Crisfield, 1981).

Numerical results for the load–CMSD relation, showing the points of onset of cracking (point A), instability (point B) and ultimate state analyzed (point C) have been plotted in Fig. 11. Good agreement with the experimental results of Arrea and Ingraffea (1981), also plotted in Fig. 11, is obtained.

In Fig. 12 the cracking pattern at the peak (point B of Fig. 11) and ultimate load (point C of Fig. 11) are shown. It is interesting to note that cracking localizes in a narrow curved band only after the peak load, for which all cracks are distributed almost vertically and form an angle of approximately 60° to the horizontal axis (see Fig. 12(a)). Excellent agreement between the localized cracking band obtained numerically and experimentally is achieved, as can be seen in Fig. 12(c).

The principal stress distributions at the onset of cracking (point A of Fig. 11) and the ultimate state (point C of Fig. 11) are shown in Fig. 13. It is worth noting the stress relaxation in the zone where cracking localizes (see Fig. 13(b)). This localization can also be clearly seen in Fig. 14, where the deformed shape of the beam (magnified 300 times) at the end of the test is shown.

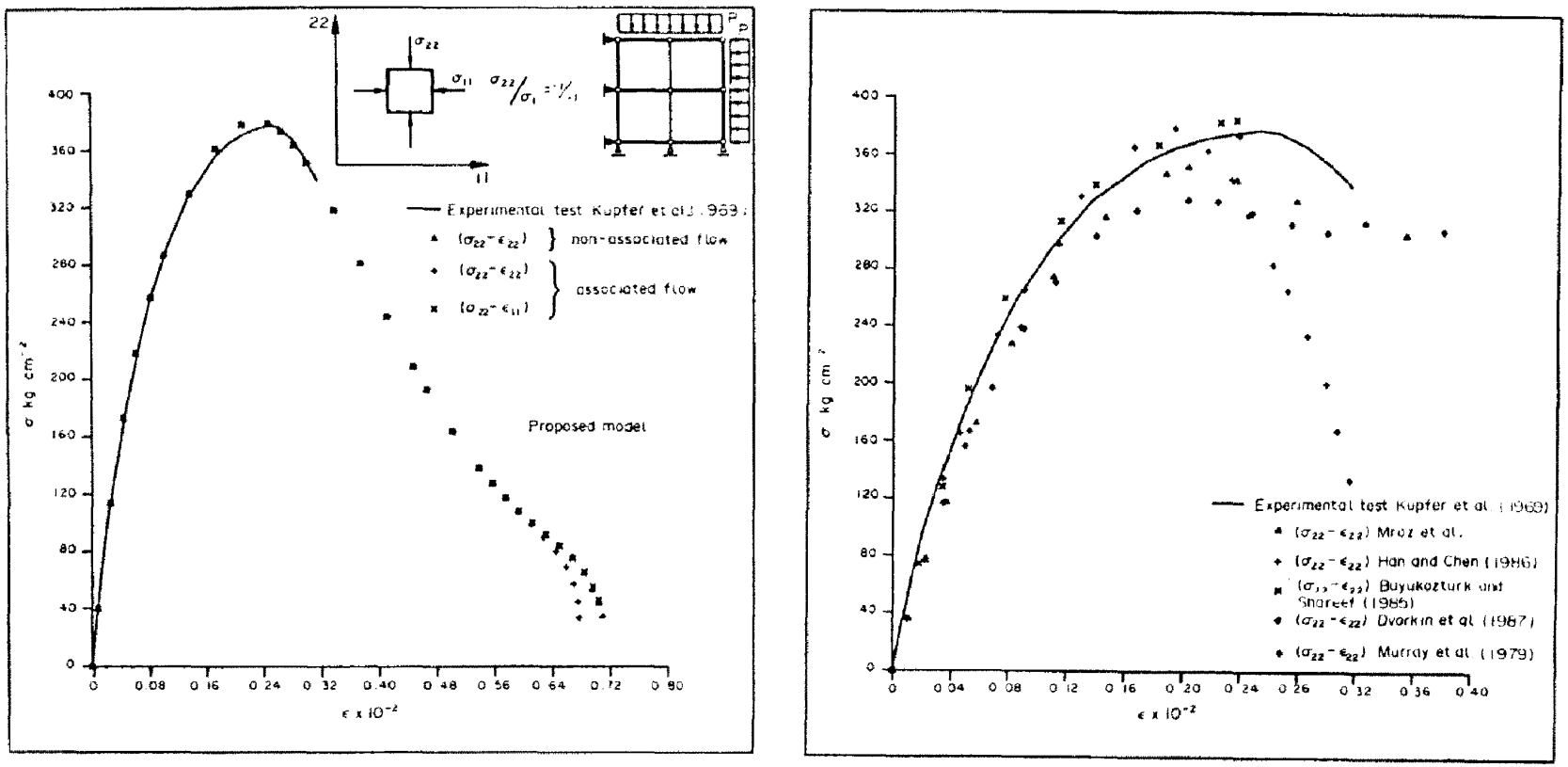

Fig. 8. Biaxial compression test. Compared stress–strain results for double symmetric compression.

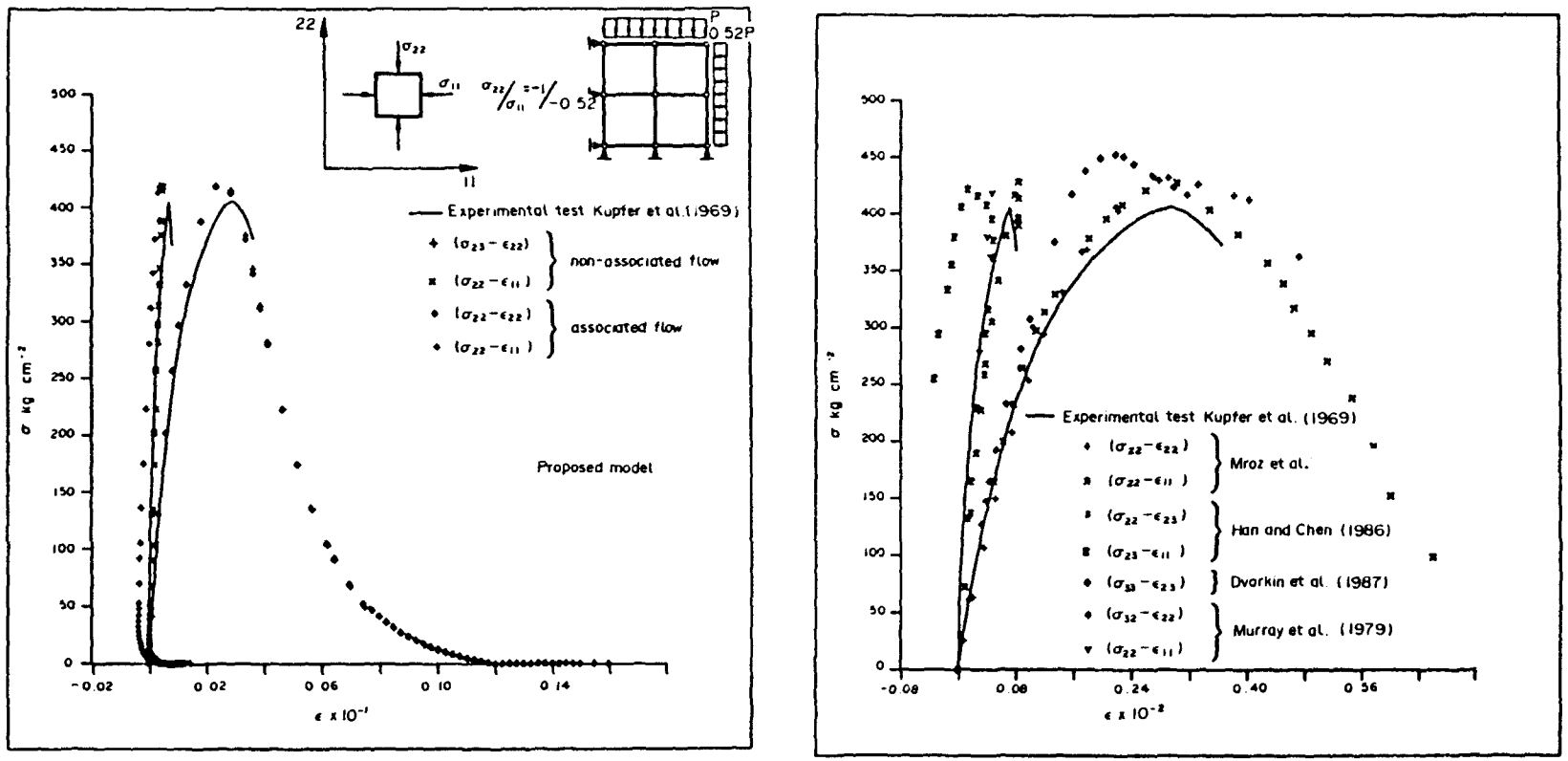

Fig. 9. Biaxial compression test. Compared stress–strain results for double non-symmetric compression.

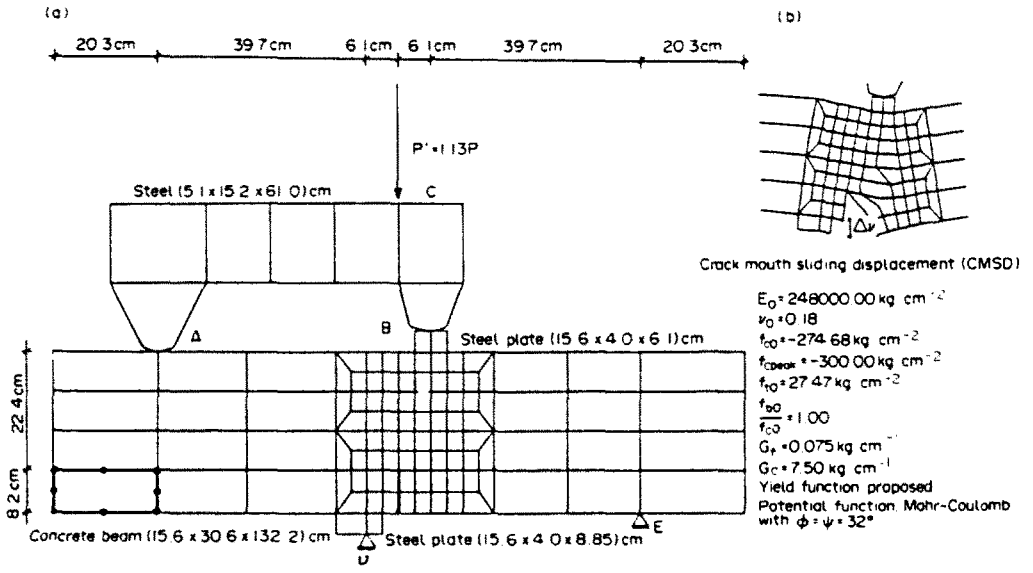

Fig. 10. (a) Notched beam. Relevant material parameters and finite element mesh. (b) Notched beam. Crack Mouth Sliding Displacement (CMSD).

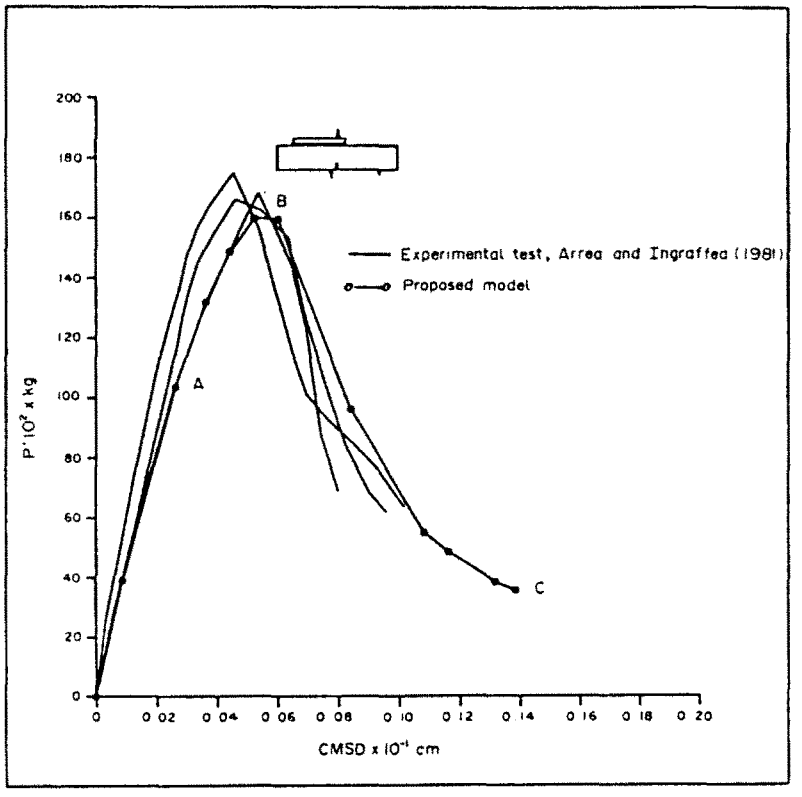

Fig. 11. Notched beam. Load–displacement curves, comparison with experimental results.

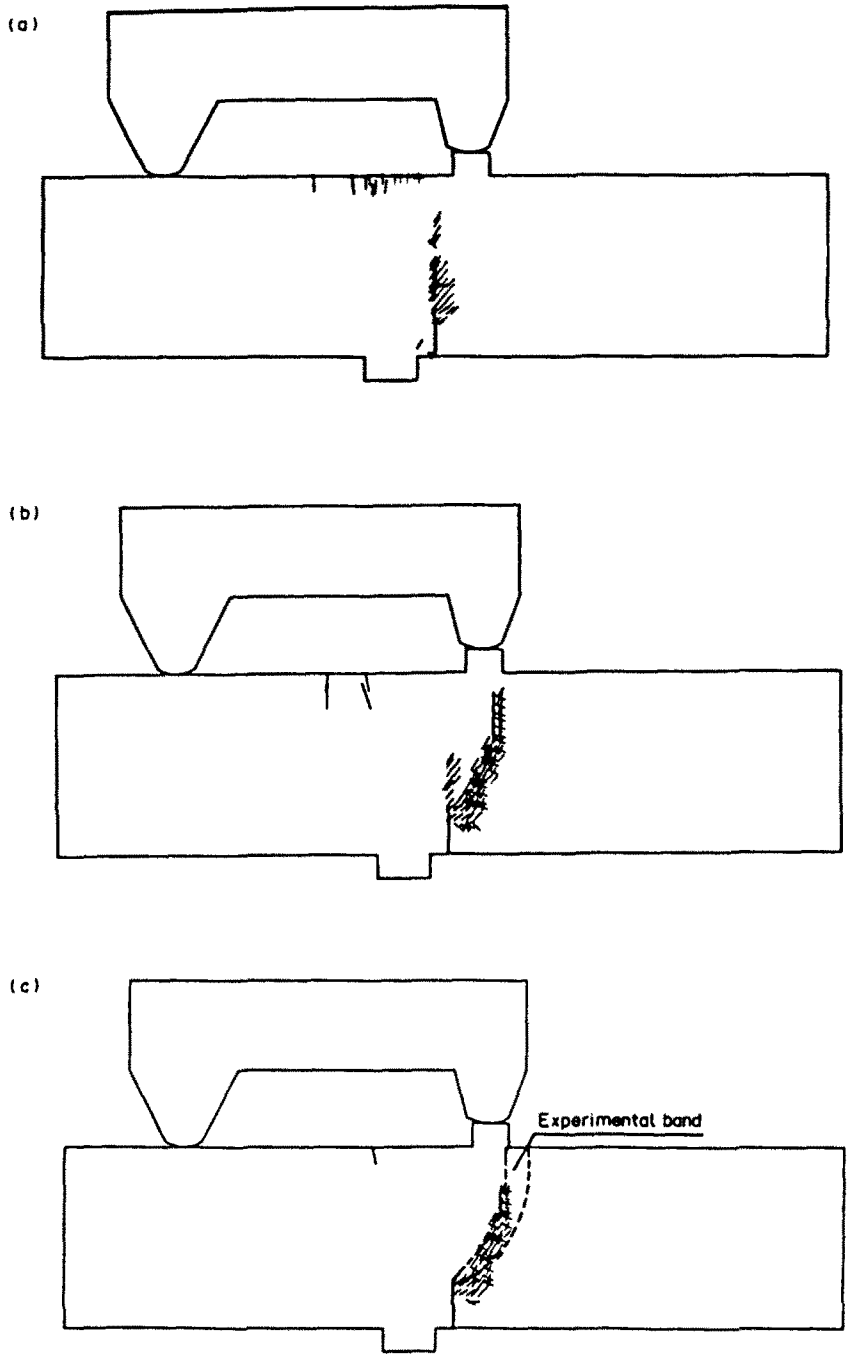

Fig. 12. Notched beam. Distribution and localization of cracking: (a) at the peak stress (B)—all cracks; (b) at the ultimate state (C)—cracks greater than 3% of the maximum crack; (c) at the ultimate state (C)—comparison with experimental results of Arrea and Ingraffea (1981)—cracks greater than 5% of the maximum crack.

5. CONCLUSIONS

The authors believe that they have demonstrated that, when appropriately applied, the classical theory of plasticity is a useful tool in the rate-independent inelastic analysis of a material, such as concrete, which by no means can be regarded as elastic-plastic in the usual sense. The significance of the result is both theoretical and practical.

On the theoretical plane, we hope to have helped to show that plasticity theory, when not interpreted too narrowly, is a very flexible model—one that can be used to describe a wide variety of behavior, including dilatancy and other non-associative phenomena, stiffness

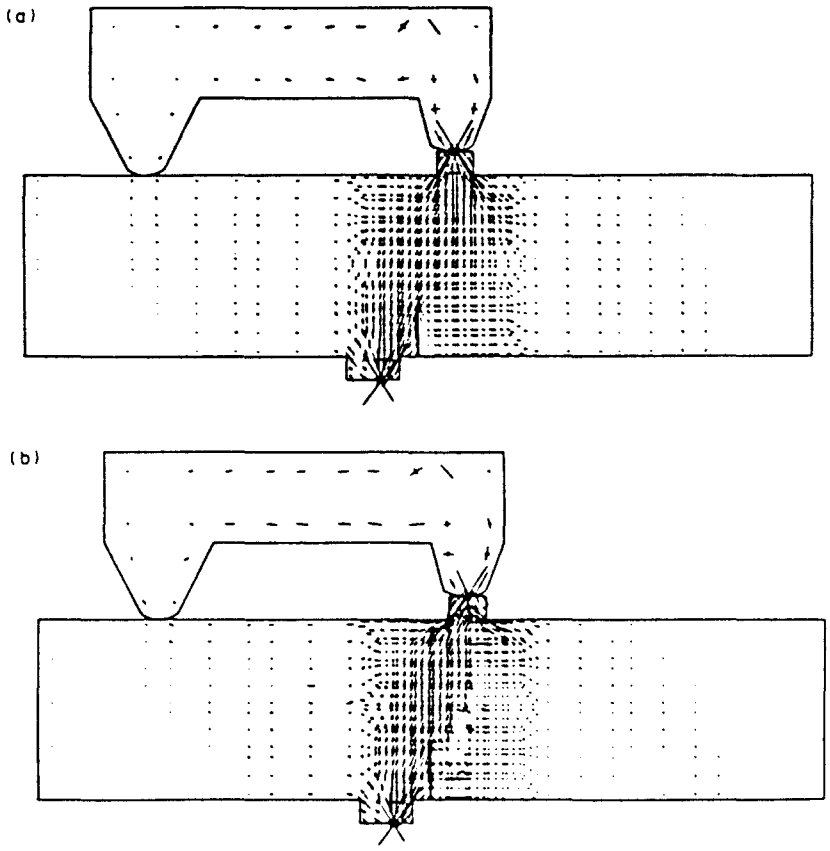

Fig. 13. Notched beam. Stress field: (a) at the elastic state (A); (b) at the ultimate state (C).

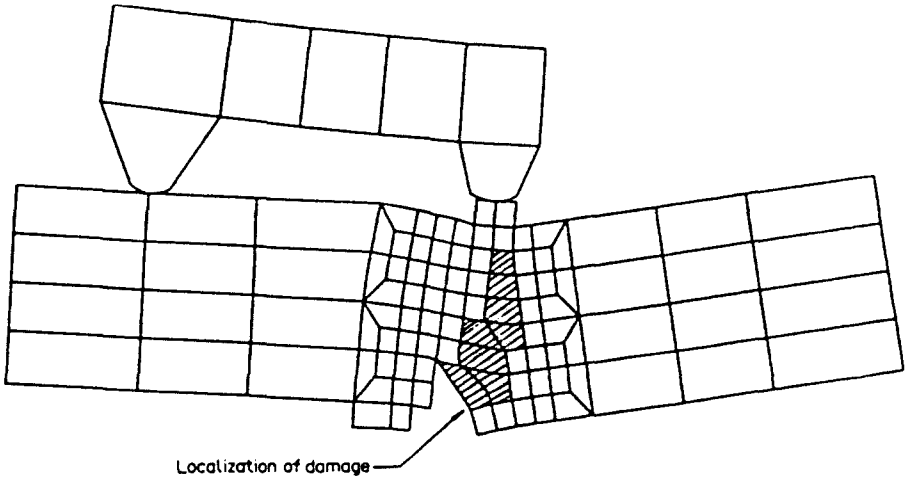

Fig. 14. Notched beam. Deformed shape at ultimate state (displacement magnified 300 times), and localization of the damage.

degradation, and others. Furthermore, it can be used to gain information about one phenomenon—cracking—which is decidedly *not* one that is usually associated with plasticity. In other words, plastic strain may be identified with any and all inelastic strain, including cracking strain.

The practical significance of our results is that plasticity theory is a rather simple model in comparison with models based on fracture mechanics or the more sophisticated versions of continuum damage mechanics. In particular, a large volume of numerical codes for the solution of problems in plasticity theory already exists, and is continually being enriched. The excellent agreement with experiment obtained in the solution of a difficult problem such as that of the notched beam shows that the potential of the present approach is great.

In future work, the authors hope to attack problems that include regions of triaxial compression through the incorporation of a cap in the yield surface.

REFERENCES

Andanaes, E., Grestle, K. and Ko, H. (1977). Response of mortar and concrete to biaxial compression. *J. Engng Mech. Div. ASCE* **103**, 515–516.

Arrea, M. and Ingraffea, A. R. (1981). Mixed mode crack propagation in mortar and concrete. Cornell University, Department of Structural Engineering, Report 81-13, Ithaca, New York.

Bažant, Z. (1986). Mechanics of distributed cracking. *Appl. Mech. Rev.* **39**, 675–705.

Bažant, Z. and Cedolin, L. (1980). Fracture mechanics of reinforced concrete. *J. Engng Mech. Div. ASCE* **106**, 1287–1306

Bažant, Z. and Oh, B. (1983). Crack band theory for fracture of concrete. *Mat. Construct. (RILEM)* **16**, 155–177.

de Borst, R. (1987). Smeared cracking, plasticity, creep and thermal loading, unified approach. *Comput. Meth. Appl. Mech. Engng* **62**, 89–110.

de Borst, R. and Nauta, P. (1984). Smeared crack analysis of reinforced concrete beams and slabs failing in shear. *Proc. Int. Conf. on Computer-Aided Analysis and Design of Concrete Structures* Vol. 1, pp. 261–273. Pineridge Press, Swansea.

Buyukozturk, O. and Shareef, S. (1985). Constitutive modeling of concrete in finite element analysis. *Comput. Struct.* **21**, 581–610.

Cedolin, L., Crutzen, R. and Dei Poli, S. (1977). Triaxial stress–strain relationship for concrete. *J. Engng Mech. Div. ASCE* **103**, EM3, 423–439.

Cervera, M., Hinton, E. and Hassan, O. (1987). Non-linear analysis of reinforced plate and shell structures using 20-node isoparametric brick elements. *Comput. Struct.* **25**, 845–870.

Chaboche, J. L. (1977). Sur l'utilisation des variables d'état interne pour la description du comportement viscoplastique et de la rupture par endommagement. ONERA, Charillon (France), T. P. No. 1977-145.

Chen, A. and Chen, W. F. (1975). Constitutive relations for concrete. *J. Engng Mech. Div. ASCE* **101**, EM4, 465–481.

Chen, W. F. (1982). *Plasticity in Reinforced Concrete*. McGraw-Hill, New York.

Crisfield, M. A. (1981). A fast incremental iterative solution procedure that handles "snap through". *Comput. Struct.* **13**, 55–62.

Crisfield, M. A. (1986). Snap-through and snap-back response in concrete structures and the dangers of under-integration. *Int. J. Num. Mech. Engng* **22**, 751–756.

Crook, A. J. L. and Hinton, E. (1987). Comparison of 2D quadrilateral finite elements for plasticity problems. *Proc. Int. Conf. Computational Plasticity* (Barcelona) (Edited by D. R. J. Owen, E. Hinton and E. Oñate) Part 1, pp. 181–195. Pineridge Press, Swansea.

Di Maggio, F. L. and Sandler, I. S. (1971). Material models for granular soils. *J. Engng Mech Div. ASCE* **97**, EM4, 935–950.

Dvorkin, E., Torrent, R. and Alvaredo, A. (1987). A constitutive relation for concrete. In *Proc. Int. Conf. Computational Plasticity* (Barcelona) (Edited by D. R. J. Owen, E. Hinton and E. Oñate) Part 2, pp. 1415–1430. Pineridge Press, Swansea.

Fardis, M. N. and Chen, E. S. (1986). A cyclic multiaxial model for concrete. *Comput. Mech.* **1**, 301–305.

Han, D. J. and Chen, W. F. (1986). Strain space plasticity formulation for hardening–softening material with elastoplastic coupling. *Int. J. Solids Structures* **22**, 935–950.

Hayhurst, D. R. and Leckie, F. A. (1973). The effect of creep constitutive and damage relationships upon the rupture time of a solid circular torsion bar. *J. Mech. Phys. Solids* **21**, 431–446.

Hillerborg, A., Modeer, M. and Petersson, P. (1976). Analysis of crack formation and crack growth in concrete by means of fracture mechanics and finite elements. *Cement Concrete Res.* **6**, 773–782.

Kachanov, L. M. (1958). Time of the rupture process under creep conditions. *Izv. Akad. Nauk S.S.S.R., Otd. Tekh. Nauk* **8**, 26–31.

Klisinski, M. and Mróz, Z. (1987). Description of inelastic deformation and degradation of concrete. Institute of Fundamental Technological Research, Internal report. Warszawa, Poland.

Kupfer, H., Hilsdorf, H. K. and Rusch, H. (1969). Behavior of concrete under biaxial stresses. *J. ACI* **66**, 656–666.

Lubliner, J. (1984). A maximum-dissipation principle in generalized plasticity. *Acta Mechanica* **52**, 225–237.

Lubliner, J. (1986). Normality rules in large-deformation plasticity. *Mech. Matls* **5**, 29–34.

Martin, J. B. and Leckie, F. A. (1972). On the creep rupture of structures. *J. Mech. Phys. Solids* **20**, 223–238.

Mills, L. L. and Zimmerman, R. M. (1970). Compressive strength of plain concrete under multiaxial loading conditions. *J. ACI* **67–10**, 802–807.

Murray, D. W., Chitnuyanondh, L., Khazal, Y. and Chung, W. (1979). Concrete plasticity theory of biaxial stress analysis. *J. Engng Mech. Div. ASCE* **105**, EM6, 989–1106.

Oliver, J. (1988). A consistent characteristic length for smeared cracking models (to appear).

Oñate, E., Oliver, J. and Bugeda, G. (1986). Finite element analysis of non-linear response of concrete dams subjected to internal loads. *Europe–US Symp. Finite Element Methods for Non-linear Problems* (Trondheim) (Edited by P. Bergan, K. J. Bathe and K. Wunderlich). Springer-Verlag, Berlin.

Oñate, E., Oller, S., Oliver, J. and Lubliner, J. (1987). A fully elastoplastic constitutive model for non-linear analysis of concrete. *Int. Conf. Num. Methods in Engng Theory and Applications*, NUMETA (Swansea) (Edited by G. Pande and J. Middleton), Martinus Nijhoff, Dordrecht, The Netherlands.

Oñate, E., Oller, S., Oliver, J. and Lubliner, J. (1988). A constitutive model of concrete based on the incremental theory of plasticity. *Engng Comput.* **5**(2).

Ottosen, N. S. (1977). A failure criterion for concrete. *J. Engng Mech. Div. ASCE* **103**, EM4, 527–535.

Podgórski, J. (1985). General failure criterion for isotropic media. *J. Engng Mech.* **111**, 188–201.

Rabotnov, Y. N. (1969). *Creep Problems in Structural Members*. North-Holland, Amsterdam.

Rashid, Y. R. (1968). Analysis of prestressed concrete pressure vessels. *Nucl. Engng Des.* **7**, 334–344.

Read, H. E. and Hegemier, G. A. (1984). Strain softening of rock, soil and concrete; a review article. *Mech. Matls* **3**, 271–294.

Richart, F. E., Brandtzaeg, A. and Brown, R. L. (1982). A study of the failure of concrete under combined compressive stresses. University of Illinois, Engineering Experiment Station, Urbana. Bulletin No. 185.

Rots, J. G., Nauta, P., Kusters, G. and Blaauwendraad, J. (1985). Smeared crack approach and fracture localization in concrete. *Heron* **30**, 1–47.

Schickert, G. and Winkler, H. (1977). Results of test concerning to multiaxial compressive stresses. *Deutscher Ausschuss für Stahlbeton*, Heft 277, Berlin, Germany.

Simo, J. C. and Ju, J. W. (1987). Strain and stress based continuum damage model. Part I: Formulation. *Int. J. Solids Structures* **23**, 281–301.

Suidan, M. and Schnobrich, W. (1973). Finite element analysis of reinforced concrete. *J. Struct. Div. ASCE* **99**, ST10, 2109–2122.

Tasuji, E., Slate, F. and Nilson, A. (1978). Stress–strain response and fracture of concrete in biaxial loading. *J. ACI* **75**, 306–312.

Willam, K. and Sobh, N. (1987). Bifurcation analysis of tangential material operators. *Int. Conf. Num. Methods Engng, Theory and Applications*, NUMETA (Swansea) (Edited by G. Pande and J. Middleton). Martinus Nijhoff, Dordrecht, The Netherlands.